Outline

Observational Evidence

DOT CaII K image close to the limb

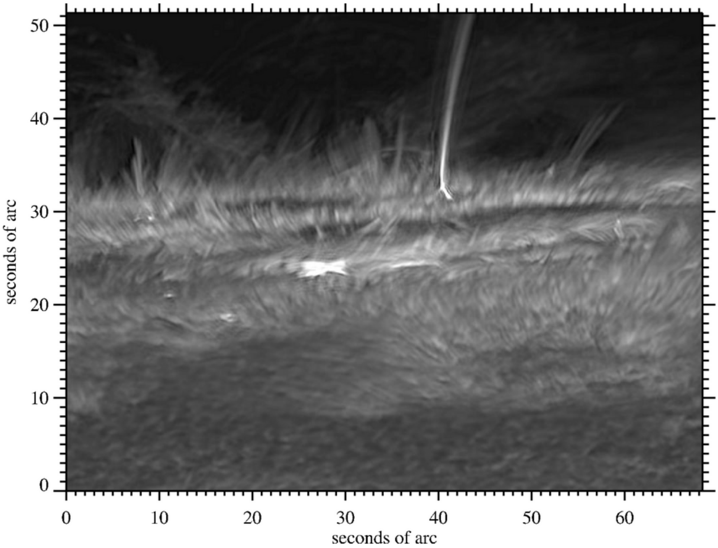

DOT Hα image

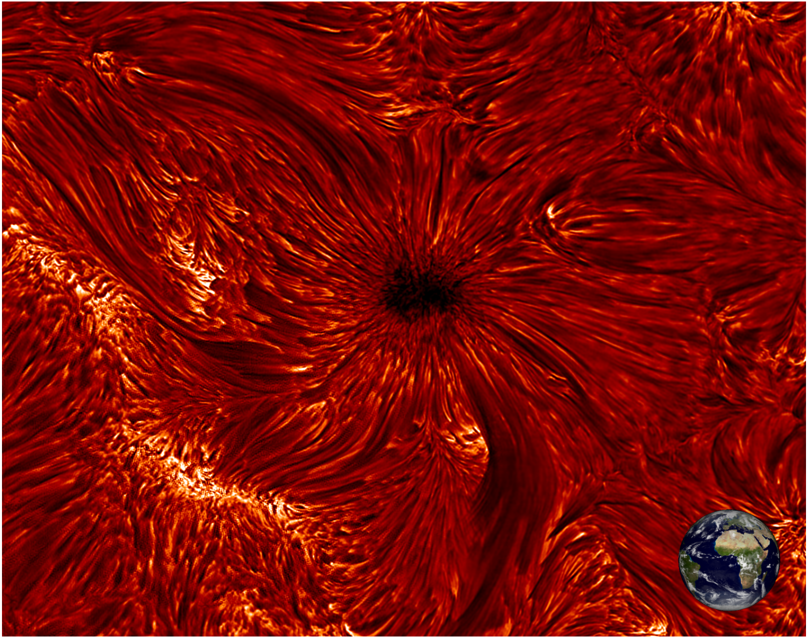

TRACE Loops

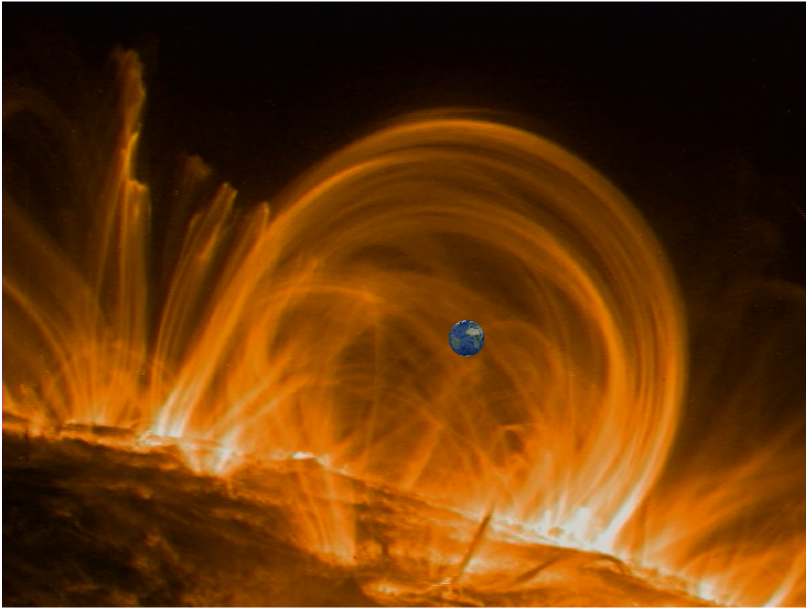

SOLIS VSM Magnetic Field Distribution

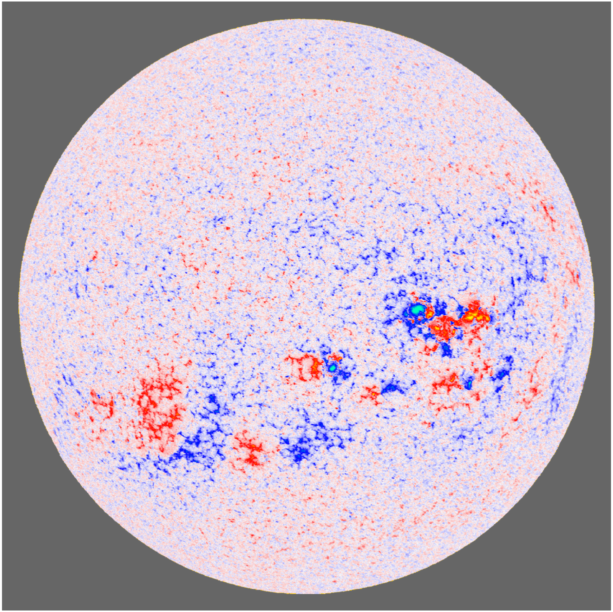

Evidence from MHD Simulations

Stein & Nordlund, Quiet Sun

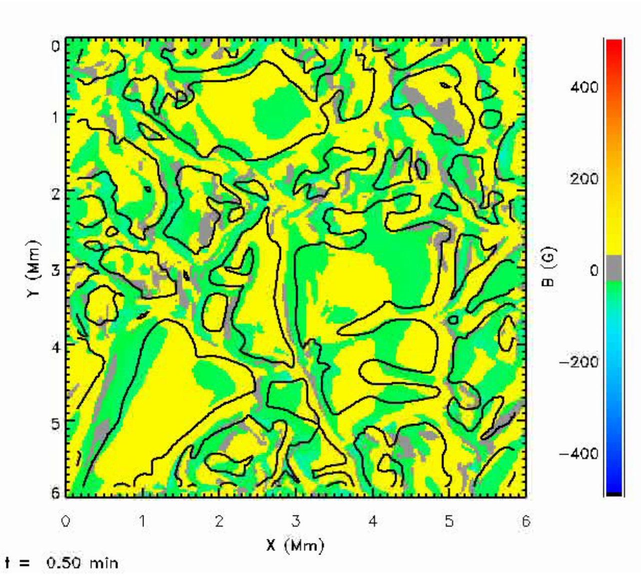

Thin Flux Tube Approximation

Force Balance

- all relative length scales are large compared to tube diameter
- neglect diffusion term in induction equation
- equation of motion

$$\rho\left(\frac{\partial\vec{v}}{\partial t}+\vec{v}\cdot\nabla\vec{v}\right)=-\nabla p+\vec{j}\times\vec{B}+\vec{F}_{\rm gravity}+\vec{F}_{\rm viscosity}$$

- magnetohydrostatic ($\vec{v}=0\Rightarrow F_{\rm viscosity}=0$)
- force balance

$$\nabla p-\vec{j}\times\vec{B}=\vec{F}_{\rm gravity}$$

- with $\mu_0\vec{j}=\nabla\times\vec{B}$ and $\vec{B}\times\left(\nabla\times\vec{B}\right)=\frac{1}{2}\nabla B^2-\left(\vec{B}\cdot\nabla\right)\vec{B}$

$$\nabla\left(p+\frac{B^2}{2\mu_0}\right)-\frac{1}{\mu_0}\left(\vec{B}\cdot\nabla\right)\vec{B}=\vec{F}_{\rm gravity}$$

Thin Flux Tube Approximation

Force Balance

- all relative length scales are large compared to tube diameter
- neglect diffusion term in induction equation
- equation of motion

$$\rho \left(\frac{\partial \vec{v}}{\partial t} + \vec{v} \cdot \nabla \vec{v} \right) = -\nabla p + \vec{j} \times \vec{B} + \vec{F}_{\text{gravity}} + \vec{F}_{\text{viscosity}}$$

- magnetohydrostatic ($\vec{v} = 0 \Rightarrow F_{\text{viscosity}} = 0$)
- force balance

$$\nabla p - \vec{j} \times \vec{B} = \vec{F}_{\text{gravity}}$$

- with $\mu_0 \vec{j} = \nabla \times \vec{B}$ and $\vec{B} \times \left(\nabla \times \vec{B} \right) = \frac{1}{2} \nabla B^2 - \left(\vec{B} \cdot \nabla \right) \vec{B}$

$$\nabla \left(p + \frac{B^2}{2\mu_0} \right) - \frac{1}{\mu_0} \left(\vec{B} \cdot \nabla \right) \vec{B} = \vec{F}_{\text{gravity}}$$

Thin Flux Tube Approximation

Force Balance

- all relative length scales are large compared to tube diameter
- neglect diffusion term in induction equation
- equation of motion

$$\rho\left(\frac{\partial\vec{v}}{\partial t}+\vec{v}\cdot\nabla\vec{v}\right)=-\nabla p+\vec{j}\times\vec{B}+\vec{F}_{\mathrm{gravity}}+\vec{F}_{\mathrm{viscosity}}$$

- magnetohydrostatic ($\vec{v}=0\Rightarrow F_{\mathrm{viscosity}}=0$)
- force balance

$$\nabla p-\vec{j}\times\vec{B}=\vec{F}_{\mathrm{gravity}}$$

- with $\mu_0\vec{j}=\nabla\times\vec{B}$ and $\vec{B}\times\left(\nabla\times\vec{B}\right)=\frac{1}{2}\nabla B^2-\left(\vec{B}\cdot\nabla\right)\vec{B}$

$$\nabla\left(p+\frac{B^2}{2\mu_0}\right)-\frac{1}{\mu_0}\left(\vec{B}\cdot\nabla\right)\vec{B}=\vec{F}_{\mathrm{gravity}}$$

Radial Force Balance

- force balance in general coordinate system

$$\nabla\left(p+\frac{B^2}{2\mu_0}\right)-\frac{1}{\mu_0}\left(\vec{B}\cdot\nabla\right)\vec{B}=\vec{F}_{\mathrm{gravity}}$$

- in cylindrical coordinates, radial component

$$\frac{\partial}{\partial r}\left(p+\frac{B^2}{2\mu_0}\right)-\frac{1}{\mu_0}\left(B_r\frac{\partial B_r}{\partial r}+B_z\frac{\partial B_r}{\partial z}-\frac{B_\phi^2}{r}\right)=0$$

- with $B_{r,\phi}=0$

$$\frac{\partial}{\partial r}\left(p+\frac{B^2}{2\mu_0}\right)=0$$

- and therefore *horizontal pressure balance*

$$p_{\mathrm{inside}}+\frac{B^2}{2\mu_0}=p_{\mathrm{outside}}$$

Radial Force Balance

- force balance in general coordinate system

$$\nabla \left(p + \frac{B^2}{2\mu_0} \right) - \frac{1}{\mu_0} \left(\vec{B} \cdot \nabla \right) \vec{B} = \vec{F}_{\text{gravity}}$$

- in cylindrical coordinates, radial component

$$\frac{\partial}{\partial r} \left(p + \frac{B^2}{2\mu_0} \right) - \frac{1}{\mu_0} \left(B_r \frac{\partial B_r}{\partial r} + B_z \frac{\partial B_r}{\partial z} - \frac{B_\phi^2}{r} \right) = 0$$

- with $B_{r,\phi} = 0$

$$\frac{\partial}{\partial r} \left(p + \frac{B^2}{2\mu_0} \right) = 0$$

- and therefore *horizontal pressure balance*

$$p_{\text{inside}} + \frac{B^2}{2\mu_0} = p_{\text{outside}}$$

Radial Force Balance

- force balance in general coordinate system

$$\nabla\left(p+\frac{B^2}{2\mu_0}\right)-\frac{1}{\mu_0}\left(\vec{B}\cdot\nabla\right)\vec{B}=\vec{F}_{\mathrm{gravity}}$$

- in cylindrical coordinates, radial component

$$\frac{\partial}{\partial r}\left(p+\frac{B^2}{2\mu_0}\right)-\frac{1}{\mu_0}\left(B_r\frac{\partial B_r}{\partial r}+B_z\frac{\partial B_r}{\partial z}-\frac{B_\phi^2}{r}\right)=0$$

- with $B_{r,\phi}=0$

$$\frac{\partial}{\partial r}\left(p+\frac{B^2}{2\mu_0}\right)=0$$

- and therefore *horizontal pressure balance*

$$p_{\mathrm{inside}}+\frac{B^2}{2\mu_0}=p_{\mathrm{outside}}$$

Plasma Beta

$$\beta = \frac{2\mu_0 p}{B^2}$$

- *Plasma* β: ratio of gas pressure to magnetic pressure
- determines whether gas pressure or magnetic field ’pressure’ is more important

Vertical Force Balance

- in the z-direction (along the field lines)

$$\frac{\partial p}{\partial z} = -\rho g$$

- with ideal gas law $\rho = \frac{\mu p}{kT}$

$$\frac{\partial p}{\partial z} = -\frac{\mu g}{kT} p$$

- pressure as a function of height z

$$p(z) = p(z_0) \exp\left(-\int_{z_0}^{z} \frac{1}{H(z')} dz'\right)$$

- with the *pressure scale height*

$$H(z) = \frac{kT}{\mu g}$$

Vertical Force Balance

- in the z-direction (along the field lines)

$$\frac{\partial p}{\partial z} = -\rho g$$

- with ideal gas law $\rho = \frac{\mu p}{kT}$

$$\frac{\partial p}{\partial z} = -\frac{\mu g}{kT} p$$

- pressure as a function of height z

$$p(z) = p(z_0) \exp\left(-\int_{z_0}^{z} \frac{1}{H(z')} dz'\right)$$

- with the *pressure scale height*

$$H(z) = \frac{kT}{\mu g}$$

Vertical Force Balance

- in the z-direction (along the field lines)

$$\frac{\partial p}{\partial z} = -\rho g$$

- with ideal gas law $\rho = \frac{\mu p}{kT}$

$$\frac{\partial p}{\partial z} = -\frac{\mu g}{kT} p$$

- pressure as a function of height z

$$p(z) = p(z_0) \exp\left(-\int_{z_0}^{z} \frac{1}{H(z')} dz' \right)$$

- with the *pressure scale height*

$$H(z) = \frac{kT}{\mu g}$$

2-D Simulations by Oskar Steiner

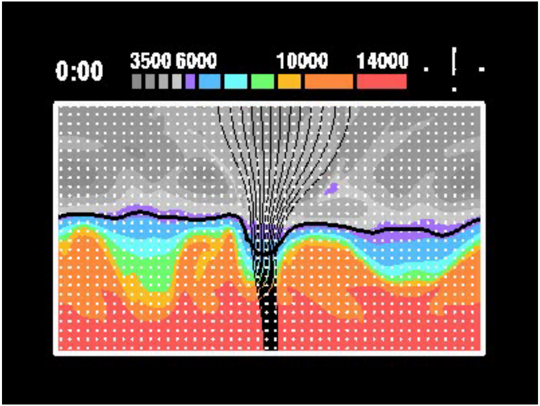

Small-Scale Magnetic Elements

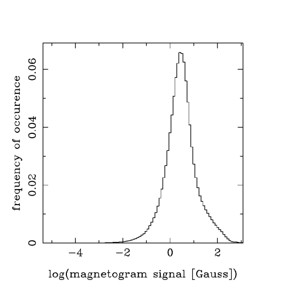

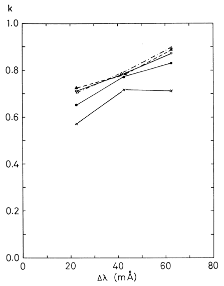

A Little History

- much of measured magnetogram signal 0-100 Gauss
- ratio of magnetograms in 2 spectral lines with “only” different Landé g-factors (line ratio technique)
- indicates high field strengths of 1000-2000 Gauss
- indicates that magnetic field is not space-filling
- *filling factor* describes fraction of resolution element filled with magnetic field

Small-Scale Magnetic Elements

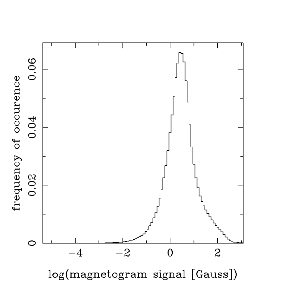

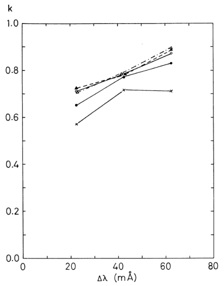

A Little History

- much of measured magnetogram signal 0-100 Gauss
- ratio of magnetograms in 2 spectral lines with “only” different Landé g-factors (line ratio technique)
- indicates high field strengths of 1000-2000 Gauss
- indicates that magnetic field is not space-filling
- *filling factor* describes fraction of resolution element filled with magnetic field

Small-Scale Magnetic Elements

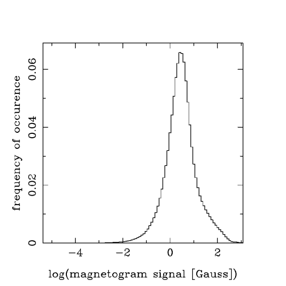

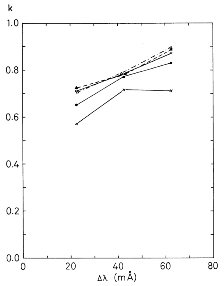

A Little History

- much of measured magnetogram signal 0-100 Gauss
- ratio of magnetograms in 2 spectral lines with “only” different Landé g-factors (line ratio technique)
- indicates high field strengths of 1000-2000 Gauss
- indicates that magnetic field is not space-filling
- *filling factor* describes fraction of resolution element filled with magnetic field

Flux vs. Field Strength

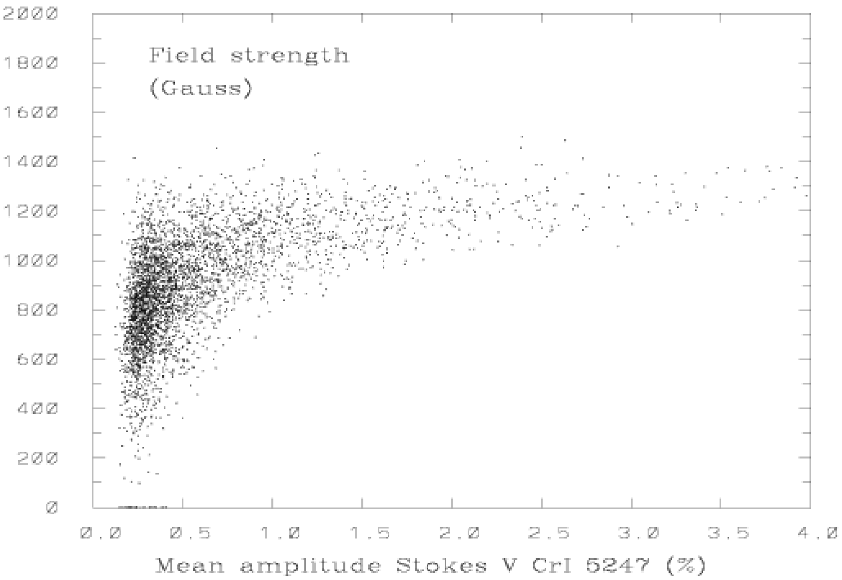

Temperature Structure

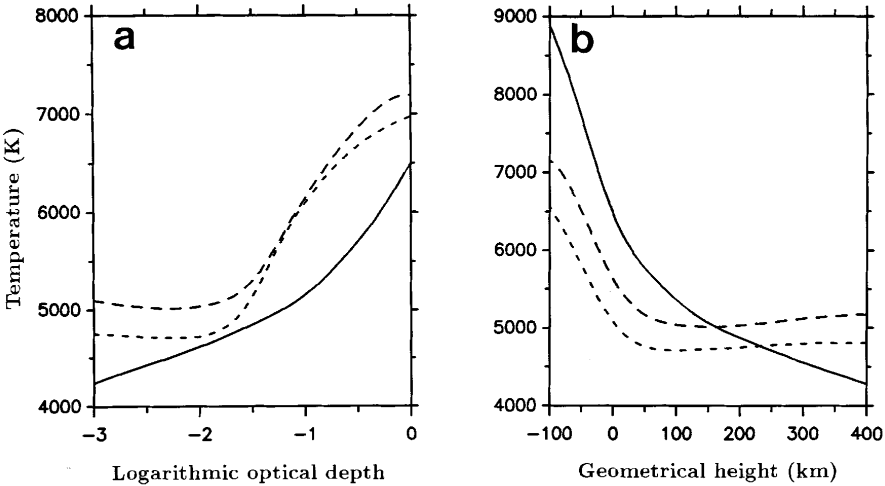

Direct Detection of Concentrated Fields

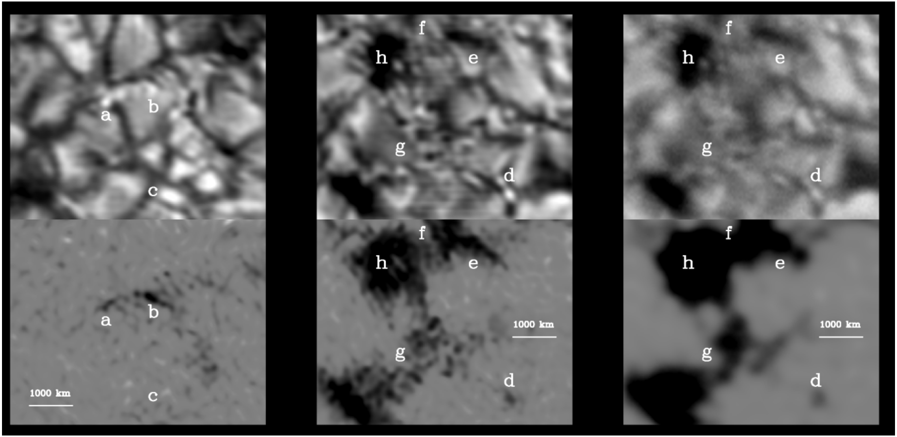

Convective Collapse

A Description

- kinetic equipartition field strength

$$\frac{B^2}{2\mu_0} = \frac{\rho}{2} v^2$$

- typical values in the photosphere: 400 G
- magnetic field inhibits convection
- reduced heating leads to lower temperature
- correspondingly higher density makes material sink

G-Band Bright Points

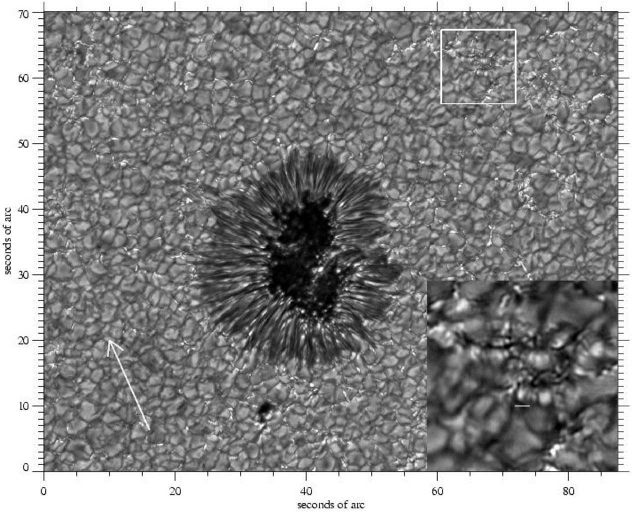

Faculae

The Sun in White Light

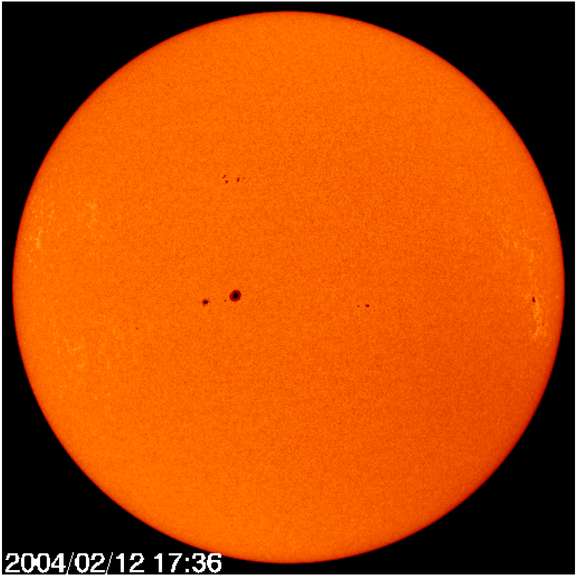

The Sun without Limb Darkening

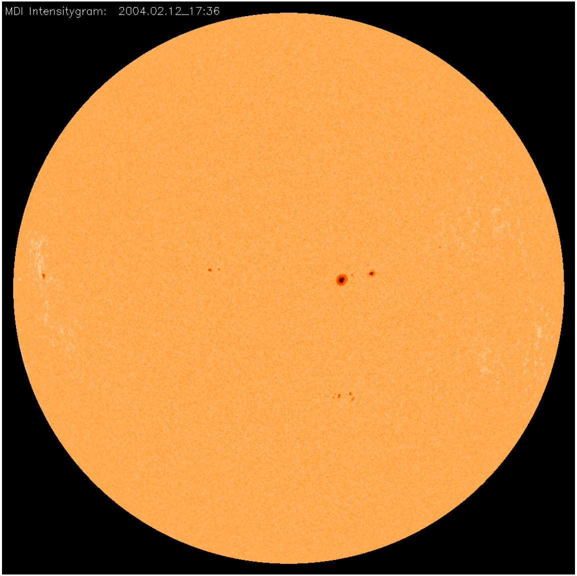

1-m Swedish Solar Telescope Observations by Lites et al. (2004)

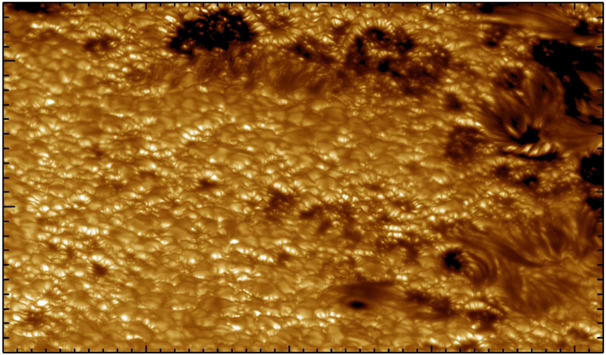

- 3-D impression when looking at images
- Faculae appear predominantly in plages
- Facular brightenings on disk-center side of granules
- Brightening can extend over about 0.5 arcsec
- Narrow, dark lanes centerward of the facular brightening

Observations by Lites et al. (2004)

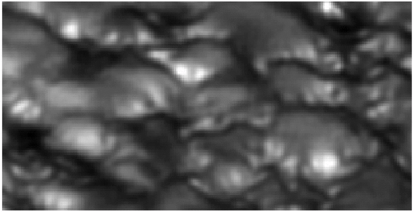

Simulation, 200 G

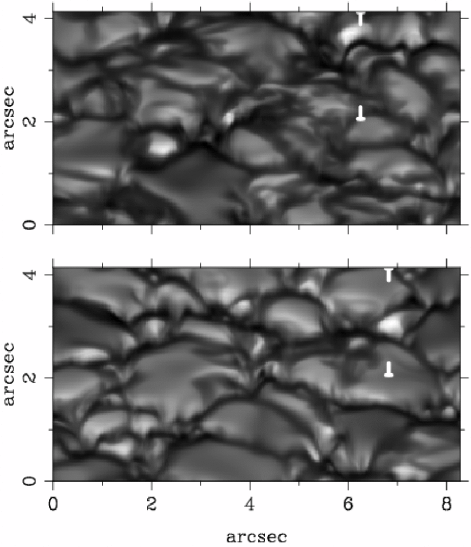

Simulation, 400 G

Simulations by Keller, Schüssler, Vögler, Zakharov, ApJL 607, L59 (2004 May 20)

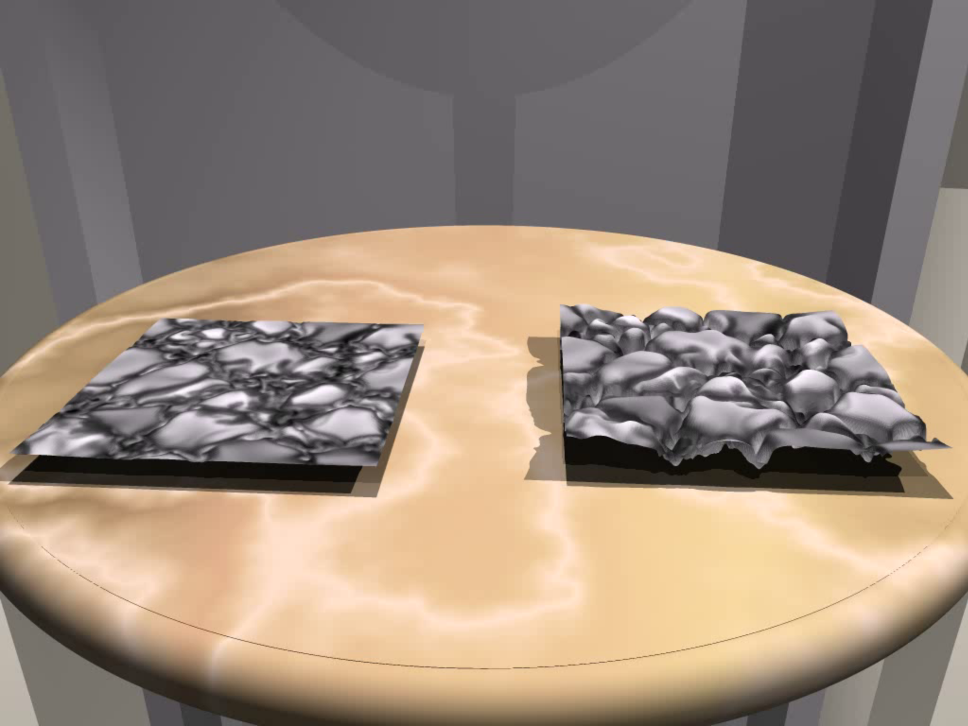

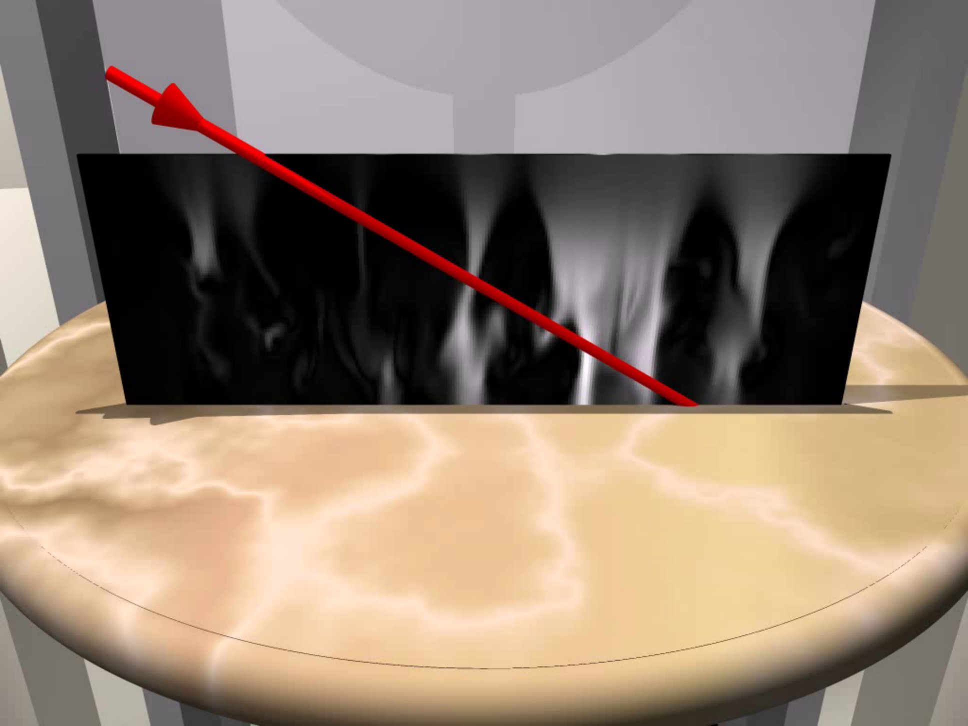

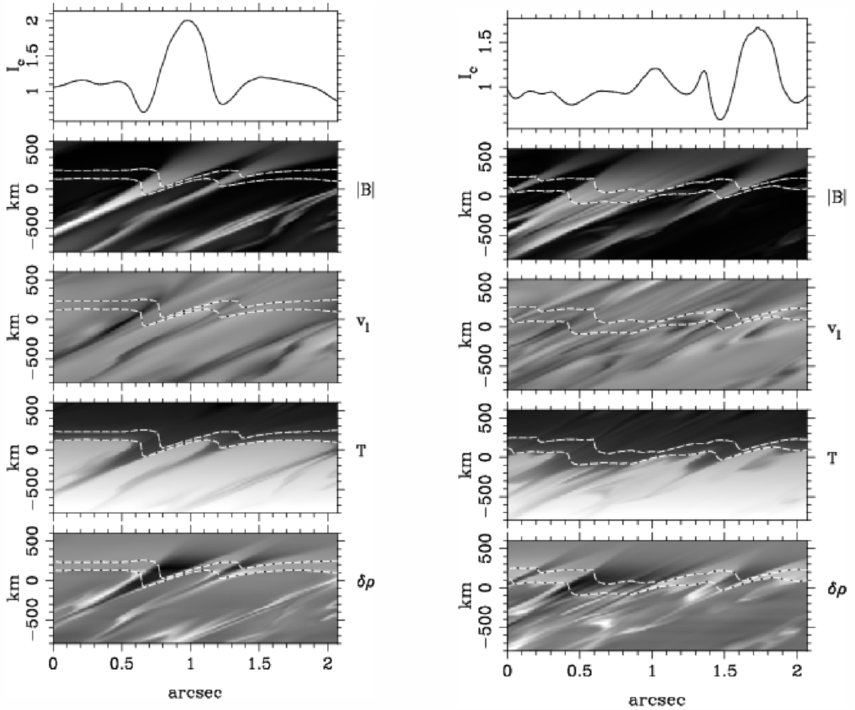

I_c
|B|
v_l
T
$\delta\rho$
km
arcsec

- Largely consistent with `bright wall' model of Spruit (1976)
- Qualitatively similar features (dark lane followed by more extended brightening) already apparent in 2D flux sheet models (e.g., Deinzer et al. 1984, Knölker & Schüssler 1988, Knölker et al. 1991)
- Expansion of flux concentrations with height and 3D geometry of granules lead to limbward extension of facular brightenings significantly in excess of the Wilson depression
- The same simple geometric effects lead to the formation of the narrow, dark lanes centerward of the facular brightenings